A&A 521, A26 (2010)
DOI: 10.1051/0004-6361/200912937

Astronomy & Astrophysics

Spectral classification and distance determination of stars in nine southern Galactic H II regions★ (Research Note)

M. C. Pinheiro, M. V. F. Copetti, and V. A. Oliveira

Laboratório de Análise Numérica e Astrofísica, Departamento de Matemática e Programa de Pós-Graduação em Física, Universidade Federal de Santa Maria, 97119-900 Santa Maria, RS, Brazil
e-mail: [pinheiro.marcio;mvfcopetti;prof.vinic]@gmail.com

Received 20 July 2009 / Accepted 15 March 2010

ABSTRACT

Aims. We attempt to identify the ionising stars and to determine the photometric distances of nine southern Galactic H II regions.
Methods. We carried out optical spectroscopy and UBV photometry of the stellar content of these objects. The distance of individual stars were obtained by spectroscopic parallax. To avoid using a fixed value for the total-to-selective extinction ratio R_V, the reddening A_V was determined directly by the colour-difference approach by comparing our V apparent magnitudes and the JHK magnitudes from the 2MASS survey with the intrinsic colour indices.
Results. As types O or B, we classified 24 of the 31 stars for which optical spectra were obtained. In particular, we identified two new O stars, one in RCW 98 and the other in RCW 99. The values of reddening obtained correspond to a mean $\langle R_V \rangle = 3.44$, which is about 10% higher than the value found for field stars. For three of the H II regions studied (Bran 186, NGC 2626, and RCW 32), the distance estimates (with errors from 25% to 50%) were based on the data obtained for only one star. For the other six objects (NGC 3503, NGC 6334, RCW 55, RCW 87, RCW 98, and RCW 99), we obtained more precise photometric distances (with a mean error of ≈18%) calculated to be the median of the parallax distances obtained for two to six different stars in each nebulae. The parallax distances of individual stars belonging to a given nebula were similar to each other, with internal errors smaller than 5%, as a consequence of the method used to derive the reddening correction A_V. The distance of 1.23 ± 0.30 kpc obtained for RCW 87 disagrees with the value of 7.6 kpc previously found.
Conclusions. The dispersion in individual distance estimates for stars in a given nebula can be significantly reduced by calculating the reddening A_V from a comparison between the V and the 2MASS JHK magnitudes instead of using $A_V = R_V E(B-V)$ with a fixed value for R_V. Therefore, more precise distances can be calculated with our proposed method.

Key words. H II regions – stars: early-type – stars: distances

1. Introduction

Several photometric and spectroscopic optical studies of the stellar content of Galactic H II regions have been published (Russeil et al. 2007, and references therein). The ionising stellar associations obscured by interstellar extinction have been intensively studied by observations in the infrared (Borissova et al. 2006). These works have been instrumental in identifying and characterizing the ionising stars, determinations of distance and age of the clusters, defining the spiral structure of the Milky Way, and, indirectly, to estimate the Galactic gradients of chemical abundances. However, the optical studies of relatively small H II regions, ionised by groups of a few stars, remain far from complete. Even the nature of some of these emission nebulae remain unclear or unconfirmed. Some of these objects have even been reclassified (Frew et al. 2006; Copetti et al. 2007; Stupar et al. 2008), but there are several objects with unverified, uncertain or even with no distance determination or classification. In this paper, we present a study of stars in nine southern Galactic H II regions with discrepant or unknown distance estimates. We performed UBV photometry and optical spectroscopy of these stars to determine their distances using the spectroscopic parallax method and, consequently, the distances of the host nebulae.

2. Observations

Direct images in the UBV bands were obtained with the 0.6 m telescope at the Observatório do Pico dos Dias (OPD), Brazil. To avoid the saturation of the brightest stars, multiple exposures were taken in each filter. Five dome flat-fields for each filter and 15 bias exposures were taken at both the beginning and the end of each night. Images of standard star fields indicated by Landolt (1992) were taken to enable a photometric calibration to be performed. Secondary standard stars catalogued by Galadí-Enríquez et al. (2000) were also used. Table 1 presents the journal of photometric observations. The CCD image field-of-view was 11′×11′. The typical seeing ranged from 1.″5 to 2.″0. The reduction followed the standard procedures for stellar CCD photometry in relatively crowed fields and was performed with IRAF. We limited the UBV photometry to stars with $V \leq 18$. Based on the colour–colour and colour–magnitude diagrams, early-type star candidates with $V \leq 14$ were selected for the spectroscopic follow-up observations. For the stars within $13 \leq V \leq 14$, we observed photometric errors of $\sigma_V = 0.019 \pm 0.011$, $\sigma_{(B-V)} = 0.026 \pm 0.015$, and $\sigma_{(U-B)} = 0.024 \pm 0.012$.

Long-slit spectrophotometric observations were carried out with the Cassegrain spectrograph attached to the 1.6 m and the 0.6 m telescopes at OPD. Table 2 presents the journal of the spectroscopic observations. A Marconi CCD of 2048 × 2048 pixels

★ Figures 1, 2 and Tables 1–3, 5 are only available in electronic form at http://www.aanda.org was used. The spectra covered the range of 4000 to 4900 Å, classically used for spectral classification of OB stars, with signal-to-noise ratios ranging from 70 to 400, with a mean value of about 200. The observation routine followed the usual procedures. Around 15 bias frames and 5 dome flat-fields were taken at the beginning and the end of each night. Spectra of a He-Ar lamp were taken before and after each object exposure to perform the wavelength calibration. The standard reduction procedure was completed with IRAF. We used the *splot* routine to normalise the continuum of the spectra to unity and to perform spectral line measurements. In each nebula, in general we observed three or four of the hottest and brightest early-type star candidates indicated by the *UBV* photometry. Since we used a long slit of $1\farcs5 \times 320''$, some secondary candidates could be observed simultaneously with the primary targets. Although we could not spectroscopically observe all candidates, the chances of missing the dominant ionising stars is low since these stars should be able to be distinguished from the relatively cool stars, unless they are hidden by local dust lanes.

3. Methods

3.1. Spectral classification

The spectra of OB stars are easily identified by the presence of He I absorption lines. The presence of He II absorption line is indicative of O stars. These were the primary criteria used to classify the stars studied here. We measured the equivalent widths of strong absorption lines of the He I, He II, and Balmer series to compare them with the values compiled by Jaschek & Jaschek (1990) and reduce our search to a few spectral types. For O stars, the He I λ4471/He II λ4541 ratio and the He I λ4388 × He II λ4686 product were also used in accordance with the prescription by Mathys (1988, 1989). Finally, we refined the spectral classification by comparing with the digital spectral atlas of Walborn & Fitzpatrick (1990), observing the specific characteristics of each spectral subtype individually described by these authors. To classify late B or cooler stars, we relied solely on the average spectral type characteristics presented by Jaschek & Jaschek (1990). The spectra of the observed OB stars are displayed in Fig. 1.

3.2. Reddening correction and distance determination

A major source of error in the photometric distances is the reddening correction, which is often estimated for the V magnitude from the colour excess $E(B-V)$ by using a mean value for the total-to-selective extinction ratio of $R_V = A_V/E(B-V) \approx 3.1$ (He et al. 1995). However, the extinction of stars inside star-forming regions can be anomalous and correspond to different, commonly far higher, values of R_V (Mathis 1990; Papaj et al. 1991; Megier et al. 1997; Patriarchi et al. 2001). Thus, the use of a "normal" value of R_V valid for field stars can introduce large errors into the estimated distances of H II regions.

In this paper, we chose to evaluate the reddening A_V directly by the colour-difference approach comparing our V apparent magnitudes and the JHK magnitudes from the 2MASS survey (Cutri et al. 2003) with the intrinsic colour indices. Using the least squares method, we fitted the relationship

$$E(\lambda - V) = A_V\,(R_L(\lambda) - 1), \tag{1}$$

where λ corresponds to the apparent magnitudes in the JHK filters, the extinction curve $R_L(\lambda) = A_\lambda/A_V$ given by Rieke & Lebofsky (1985), and the intrinsic colours $(J-V)_0$, $(H-V)_0$, and $(K-V)_0$ from Wegner (1994).

The extinction law is approximately described by a power law with a fixed exponent β. However, Fitzpatrick & Massa (2009) argued that there may not be a universal law for the extinction curve, which should depend instead on the sight line. The power law approximation would remain valid, but would different values of β for different sight lines (and wavelength ranges). Based on the dispersion of ≈20% in the values of β fitted by Fitzpatrick & Massa (2009), we found that the usual adoption of a extinction curve with a fixed exponent would cause errors in distance of ≈15%.

The heliocentric photometric distance d was calculated adopting the calibration of the absolute magnitude M_V as a function of the spectral type and luminosity class given by Russeil (2003). The error in distance was estimated to be

$$\sigma_d = \frac{\ln 10}{5}\, d\, \sqrt{\sigma_V^2 + \sigma_{M_V}^2 + \sigma_{A_V}^2}\,, \tag{2}$$

where σ_V, σ_{M_V} and σ_{A_V} are the uncertainties in apparent and absolute magnitudes and in reddening, respectively. The dominant sources of the errors in distance are uncertainties in the absolute magnitude adopted and in reddening, since $0.1 \lesssim \sigma_{A_V} \lesssim 1.0$, and $\sigma_{M_V} \approx 0.5$ (Russeil 2003), whereas $\sigma_V \lesssim 0.05$.

4. Results and discussions

Table 3 presents the results of our spectroscopic and photometric studies of individual stars. Columns 1–3 provide the identifications of the stars studied in this paper, in the 2MASS survey, and in the Simbad database, respectively. Columns 4 and 5 indicate the stellar spectral classifications from this paper and from the literature, respectively. Columns 7 to 12 show the observed V magnitude and $(B-V)$ colour, the colour excess $E(B-V)$, the calculated reddening A_V, the total-to-selective extinction ratio R_V, and the corresponding heliocentric photometric distance d, respectively.

Table 4 indicates the photometric distance of each H II region studied, which corresponds to the median of the values obtained for n individual stars. For those objects in which more than one star was studied, the error estimates correspond to $(\sum \sigma_i^2/n(n-1))^{1/2}$, where σ_i is the error in the distance for each star. These errors are in the range of 13% to 50%, and are about 15% for the objects with three or more stars studied. The standard deviations in the distances measured for different stars in a given nebula are much smaller, varying from 1% to 13%, but are unrealistic error bounds, serving only to assess the internal consistency of the distance determinations of individual stars, because systematic errors are not taken into account.

To test the completeness of the sample of ionising stars identified in each nebula, we indicate and compare in Table 5, the Hβ extinction data for both the nebulae and the stars, i.e., $C(\mathrm{H}\beta)$, and for the Lyman continuum photon flux, N_c. Columns 3–5 provide the values of $C(\mathrm{H}\beta)$ calculated from the stellar photometry, which are given by $C(\mathrm{H}\beta) = 1.5E(B-V)$, from the nebular H$\gamma$/H$\beta$ line ratio, and from the ratio of the radio continuum flux density to the Hβ flux, respectively. Columns 6–8 provide the values of N_c obtained from the summed ionising photon rates of individual stars, from the observed Hβ line fluxes, and from the radio continuum flux densities at 2.7 GHz (Paladini et al. 2003), respectively. We adopted the values of N_c found by Schaerer & de Koter (1997) for stars of different spectral types. The integrated Hβ line fluxes from Copetti (2000) were adopted for all objects apart from Bran 186, for which the extrapolation given by Acker et al. (1991) was used. As an additional compatibility test between the nebular and stellar properties, Table 5 also compares the various spectral types of the identified ionising stars

Table 4. Heliocentric distances for the studied H II regions.

H II region	n	d (kpc)	
		This work	Literature
Bran 186	1	3.05 ± 1.45	
NGC 2626	1	1.20 ± 0.34	0.95 [1], 1.25 [2]
RCW 32	1	0.67 ± 0.17	0.72 [2], 0.70 [3], 0.77 [4]
NGC 3503	5	2.85 ± 0.37	2.6 [1], 3.5 [5], 4.2 [6]
RCW 55	7	4.36 ± 0.46	4.3 [7], 3.08 [8]
RCW 87	2	1.23 ± 0.30	7.6 [9]
RCW 98	3	2.61 ± 0.46	2.87 [2], 3.0 [7], 2.8 [10]
RCW 99	2	3.55 ± 1.82	3.54 [7]
NGC 6334	6	1.75 ± 0.26	2.10 [7], 2.3 [11], 1.74 [12]

References. [1] Herbst (1975), [2] Crampton & Fisher (1974), [3] Georgelin et al. (1973), [4] Vogt & Moffat (1975), [5] Kharchenko et al. (2005), [6] Moffat & Vogt (1975), [7] Avedisova & Kondratenko (1984), [8] Brand & Blitz (1993), [9] Borissova et al. (2006), [10] Yamaguchi et al. (1999), [11] Walborn (1982), [12] Neckel (1978).

and the emission line ratio [O III]λ4959/Hβ, which roughly assesses the degree of excitation of the nebula. With the exception of one object, RCW 87, the identified ionising stars are capable of maintaining the ionisation of their respective nebulae. The line ratios [O III]λ4959/Hβ observed are typical of nebulae excited by early B or late O-type stars. In the following, we comment on some of the objects studied.

NGC 6334. This is a 50′ complex of H II regions. We used it to test the distance determination based on A_V obtained by comparing the V and JHK magnitudes. We identified the B0.5 V star LS 4087 as the ionising source of the component Gum 64a and reanalysed the data obtained by Walborn (1982) for five other stars in different components of the complex. The mean distance of 1.75 kpc obtained for these six stars exhibited an internal error of only 3.8%. This distance is 24% lower than the value obtained by Walborn (1982) using a fix value of $R_V = 3.0$, because of the higher values of A_V that we found (corresponding to a mean of $\langle R_V \rangle = 3.5$).

NGC 3503. The main sources of ionisation of this H II region are one B0 V and three B2 V stars found at the centre of the compact open cluster Pismis 17. The distance estimates for these four stars are remarkably similar, with a mean deviation of less than 2%.

Bran 186. This is a 3′ roughly round low surface brightness emission nebula discovered by Kohoutek (1971) on a R plate of the Palomar Sky Survey, designated as PN K 2-15, and classified as a possible planetary or diffuse nebula. It also appeared as the suspected planetary ESO 260-8 on the ESO/Uppsala survey of the ESO (B) atlas by Holmberg et al. (1978, the original identification was 260-PN?08) and PN G263.2+00.4 on the Strasbourg-ESO Catalogue of Galactic Planetary Nebulae by Acker et al. (1992). Based on a spectroscopic analysis, Kohoutek & Pauls (1994) included PN K 2-15 among their list of confirmed planetary nebulae. However, the status of H II region for Bran 186 was strongly indicated by the detection of a site of recent star formation at the eastern border of the optical nebula, 1.8′ from the centre, towards the source IRAS 08470-4243, which has IRAS colours typical of ultracompact H II regions. An embedded star cluster, named [DBS2003] 23, was detected by the 2MASS survey (Dutra et al. 2003) at the position of IRAS 08470-4243.

We found that the B0 V star Bran 186-3 is the ionisation source of Bran 186. A star of this spectral type is compatible with the inferred ionising photon rate and the low degree of excitation of the nebula. In our nebular spectra, we measured [O III]λ4959/H$\beta \lesssim 0.17$ and found no helium emission lines, indicating that most of the oxygen is single ionised and the helium is almost neutral.

NGC 2626. This is a bright reflection nebula located at the southwest edge of the large (100′ × 100′) H II region RCW 27 and illuminated by the B1 V star CD-40 4427. For CD-40 4427, we estimated a distance of 1.20 ± 0.34 kpc. For the emission-line star CPD-40 2663 located towards the dark cloud region 4′ from the centre of NGC 2626, a distance of 1.26 kpc was obtained by Gahm & Malmort (1980). For HD 73882, which is the exciting star of RCW 27, a distance of 1.13 kpc was estimated by Georgelin & Georgelin (1970a) and 1.04 kpc by Crampton & Fisher (1974). The similarity between the distance estimates for these three stars indicates that RCW 27, NGC 2626, and the nearby star-formation area are part of the same system.

RCW 55. We classified one star as O8 V and another six stars as type B. Although the distance estimates for these seven stars are, within the errors, compatible to one another, we may be tempted to consider that there are two superimposed stellar groups, one at 4.65±0.74 kpc and another at 2.87±0.59 kpc. However, this idea is not supported by the values of $E(B-V)$, which are indicative of similar interstellar extinction.

In Table 5, we see that the total rate of ionising photon from the identified stars is much higher (by two orders of magnitude) than that needed to maintain the ionisation of the nebula. This discrepancy may be caused by a massive leakage of Lyman continuum radiation from the nebula or else by an underestimation of the ionising luminosity required. The Hβ emission line flux used in this calculation was measured in a circular aperture with 1′40″ of diameter centred on the star RCW 55-7, located in the middle of the bright core of the nebula, while fainter emission extends across a diameter of about 10′. However, a rough extrapolation of the ionising photon flux to the whole nebula based on an image from the AAO/UKST Hα survey (Parker et al. 2005) still indicates a value lower (by an order of magnitude) than that from the stars. It is possible than some of the hot stars identified towards RCW 55 are not ionising the nebula, even though they belong to the same stellar association. It is noticeable that the bright nebular core surrounds the B1 V stars RCW 55-3 and RCW 55-7 and not the O8 V star RCW 55-4, the hottest star towards RCW 55. These two B1-type stars are capable of providing the needed ionising radiation.

RCW 87. We classified two 11th magnitude stars as B4 V and B9 III. According to Table 5, these stars are not the main ionising stars of this nebula. Neither of them is in the brightest part of the nebula, where only three or more magnitudes fainter stars are found. The mean distance of these two stars is $d = 1.23 \pm 0.30$ kpc. Figure 2 shows the $B-V$ vs. V colour–magnitude diagram for RCW 87. The bulk of stars towards RCW 87 correspond to points in this diagram that are compatible with main sequence stars at the distance and reddening calculated for the two stars that were spectroscopically observed. The stars in the embedded cluster [BDB2003] G320.15+00.79 (Bica et al. 2003), located towards the brightest part of RCW 87, are detached from the rest. However, assuming that these are also main sequence stars, we obtained from the $U-B$ vs. $B-V$ diagram a reddening of $A_V = 6.8$, leading us to conclude that they are at the same distance as the other stars. Our photometric spectral classification study indicates that there are one B1 and three B3 stars in

[BDB2003] G320.15+00.79, which could maintain with the ionisation of this nebula.

Borissova et al. (2006) presented a near and mid-infrared study of the star cluster [BDB2003] G320.15+00.79. Based on the spectroscopic parallax of the brightest star of this cluster in the near infrared, which was classified as a K0.5 II type star, these author determined a distance of 7.6 kpc for RCW 87. However, using their distance and reddening of $A_V = 10.9$ we calculate an ionising photon rate of $\log N_c = 51.5$ s^{-1}, which is unrealistically high since it would place RCW 87 among the brightest H II regions of the Galaxy and indicate that this object should be more conspicuous at radio frequencies.

RCW 99. This is a bright 4′ nebula. Avedisova & Kondratenko (1984) attributed this to a distance of 3.54 kpc, a value almost identical to that of 3.55 kpc found in this papers. However, these authors based their result on five stars outside the nebulosity, 28′ to 40′ far from its centre. The similarity between the distances of RCW 99 and stars in the field is probably not coincidental but an indication that these stars belong to same large stellar association. No hot star towards the nebulosity had been previously identified. We discovered an O7 III star (RCW 99-1) and a B2 V star (RCW 99-2) in this object.

5. Summary

We carried out spectroscopic and photometric observations of the stellar content of 9 nine southern Galactic H II regions to identify ionising stars and to determine the photometric distances of the nebulae. The distance of individual stars were obtained by spectroscopic parallax. To avoid using a fixed value for the total-to-selective extinction ratio R_V, the reddening A_V was determined directly by applying the colour-difference approach comparing our V apparent magnitudes with the JHK magnitudes from the 2MASS survey. Our main findings are:

1. We classified 24 of the 31 stars for which optical spectra were obtained as types O or B. We identified two new O stars: RCW 98-2 (O9.5 V) and RCW 99-1 (O7 III).
2. For three of the H II regions studied (Bran 186, NGC 2626, and RCW 32) the distance estimates (with errors from 25% to 50%) were based on the data obtained for only one star. For the other six objects (NGC 3503, NGC 6334, RCW 55, RCW 87, RCW 98, and RCW 99), we obtained more precise photometric distances (with a mean error of ≈18%) calculated to be the median values of the parallax distances obtained for two to six different stars in each nebulae.
3. The parallax distances of individual stars belonging to a given nebula were found to be similar to each other, having an internal dispersion of less than 5%. This is a consequence of the method used to derive the distance, which is based on an estimation of the reddening correction A_V derived by comparing our V magnitude with the JHK magnitudes from 2MASS, and assumes that the total-to-selective extinction ratio of R_V is a free parameter.
4. The common procedure of adopting a fixed value for R_V to calculate A_V from the colour excess $E(B-V)$ would have considerably increased the scatter in the distance estimates and should be employed with restraint in the case of star-forming regions.
5. The mean $\langle R_V \rangle = 3.46$ was about 10% higher than the value found for field stars. Stars located more centrally in the nebula tend to exhibit higher values of R_V.
6. For RCW 87, the distance of 1.23 ± 0.30 kpc obtained in this paper disagrees with the photometric distance of 7.6 kpc estimated by Borissova et al. (2006) based on a near infrared study of a K0.5 II type star. Additional observations are needed to resolve this discrepancy.

Acknowledgements. This work was supported by the Brazilian agencies CAPES and CNPq. We wish to thank the staff of the Laboratório Nacional de Astrofísica for their assistance during the observations.

References

Acker, A., Raytchev, B., Stenholm, B., & Tylenda, R. 1991, A&AS, 90, 89
Acker, A., Marcout, J., Ochsenbein, F., Stenholm, B., & Tylenda, R. 1992, Garching: European Southern Observatory
Avedisova, V. S., & Kondratenko, G. I. 1984, Nauchnye Informatsii, 56, 59
Bica, E., Dutra, C. M., & Barbuy, B. 2003, A&A, 397, 177
Borissova J., Ivanov V. D., Minitti D., & Geisler D. 2006, A&A, 455, 923
Brand, J., & Blitz, L. 1993, A&A, 275, 67
Buscombe, W. 1969, MNRAS, 144, 31
Copetti, M. V. F. 2000, A&AS, 147, 93
Copetti, M. V. F., Oliveira, V. A., Riffel, R., Castañeda, H. O., & Sanmartim, D. 2007, A&A, 472, 847
Corben, P. M., Carter, B. S., Banfield, R. M., & Harvey, G. M. 1972, MNRAS Afr., 31, 7
Crampton, D. 1971, AJ, 76, 260
Crampton, D., & Fisher, W. A. 1974, Publ. Dom. Astrophys. Obs., 14, 283
Cutri, R. M., et al. 2003, 2MASS All-Sky Point Source Catalog
Denoyelle, J. 1977, A&AS, 27, 343
Dutra, C. M., Bica, E., Soares, J., & Barbuy, B. 2003, A&A, 400, 533
Fitzpatrick, E. L., & Massa, D. 2009, ApJ, 699, 1209
Frew, D. J., Parker, Q. A., & Russeil, D. 2006, MNRAS, 372, 1081
Gahm, G. F., & Malmort, A. M. 1980, A&A, 82, 295
Galadí-Enríquez, D., Trullols, E., & Jordi C. 2000, A&AS, 146, 169
Georgelin, Y. P., & Georgelin, Y. M. 1970a, A&A, 6, 349
Georgelin, Y. P., & Georgelin, Y. M. 1970b, A&AS, 3, 1
Georgelin, Y. M., Georgelin, Y. P., & Roux, S. 1973, A&A, 25, 337
He, L., Whittet, D. C. B., KilKenny, D., & Spencer Jones, J. H. 1995, ApJS, 101, 335
Herbst, W. 1975, AJ, 80, 212
Holmberg, E. B., Lauberts, A., Schuster, H.-E., & West, R. M. 1978, A&AS, 31, 15
Houk, N. 1978, Michigan Catalog of Two-dimensional Spectral Types for the HD stars (Ann Arbor, MI: Dept. of Astronomy, University of Michigan), QB6.H77
Jaschek, C., & Jaschek, M. 1990, The classification of stars (Cambridge University Press)
Kharchenko, N. V., Piskunov, A. E., Roeser, S., Schilbach, E., & Scholz R.-D. 2005, A&A, 438, 1163
Kohoutek, L. 1971, A&A, 13, 493
Kohoutek, L., & Pauls, R. 1994, Astron. Nachr., 315, 409
Landolt, A. U. 1992, AJ, 104, 340
Mathis, J. S. 1990, ARA&A, 28, 37
Mathys, G. 1988, A&AS, 76, 427
Mathys, G. 1989, A&AS, 81, 237
Megier, A., Krelowski J., Patriarchi, P., & Aiello, S. 1997, MNRAS, 292, 853
Moffat, A. F. J., & Vogt, N. 1975, A&AS, 20, 125
Munch, L. 1955, Boletin de los Observatorios Tonantzintla y Tacubaya, 2, 28
Neckel, T. 1978, A&A, 69, 51
Neckel, Th., & Chini, R. 1981, A&AS, 45, 451
Paladini, R., Burigana, C., Davies, R. D., et al. 2003, A&A, 397, 213
Papaj, J., Wegner, W., & Krelowski, J. 1991, MNRAS, 252, 403
Parker, Q. A., Phillips, S., Pierce, M. J., et al. 2005, MNRAS, 362, 689
Patriarchi, P., Morbidelli L., Perimotto M., & Barbaro G. 2001, A&A, 372, 644
Rieke G. H., & Lebofsky M. J. 1985, ApJ, 288, 618
Russeil, D. 2003, A&A, 397, 133
Russeil, D., Adami, C., & Georgelin, Y. M. 2007, A&A, 470, 161
Stock, J. 1984, Rev. Mex. Astron. Astrofis., 9, 127
Stupar, M., Parker, Q. A., & Filipović, M. D. 2008, MNRAS, 390, 1037
Schaerer, D., & de Koter, A. 1997, A&A, 322, 598
Vogt, N., & Moffat, A. F. J. 1975, A&A, 45, 405
Walborn N. R. 1982, AJ, 87, 1300
Walborn N. R., & Fitzpatrick, E. L. 1990, PASP, 102, 379
Wegner W. 1994, MNRAS, 270, 229
Yamaguchi, R., Saito, H., Mizuno, N., et al. 1999, PASJ, 51, 791

Pages 5 to 9 are available in the electronic edition of the journal at http://www.aanda.org

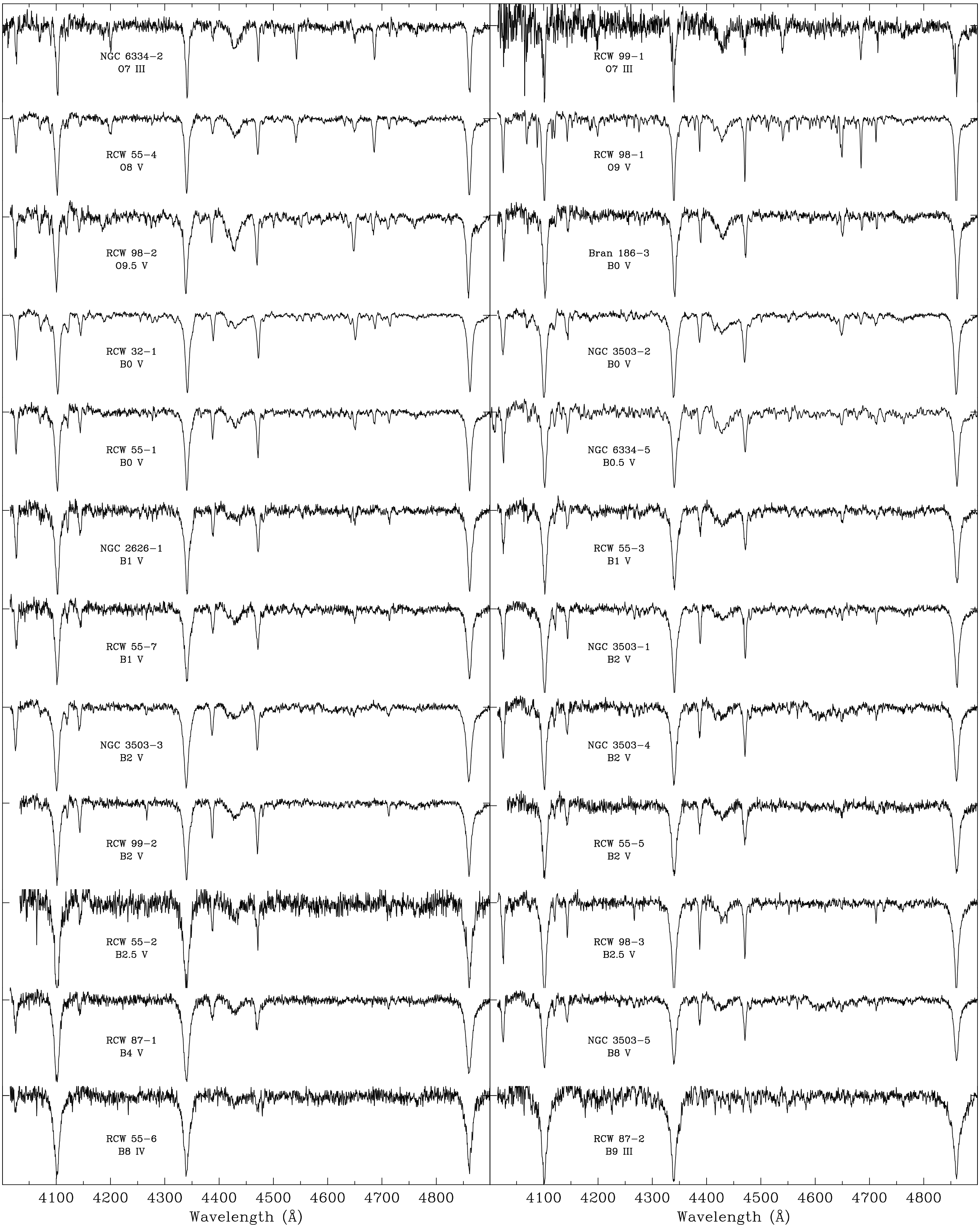

Fig. 1. Spectra of the OB stars.

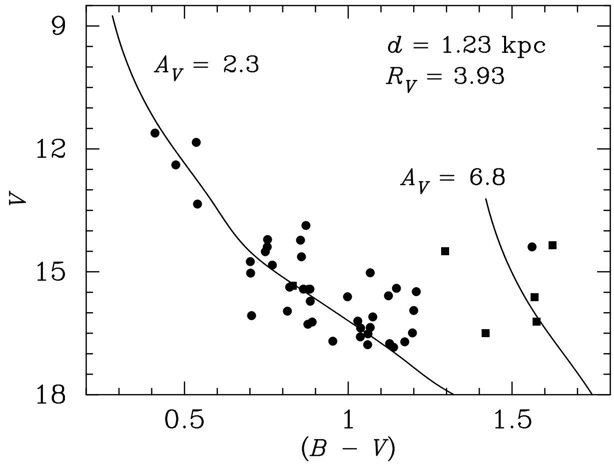

Fig. 2. The colour–magnitude diagram for RCW 87. The squares correspond to stars towards the embedded star cluster [BDB2003] G320.15+00.79 and the circles to the other stars. Also shown are the main sequence loci corresponding to a distance of 1.23 kpc and two different reddening, A_V = 2.3 and A_V = 6.8.

Table 1. Journal for photometric observations.

H II region	Exposure (s)			Date
	U	*B*	*V*	
RCW 55	3 × 500	4 × 90	3 × 60	2007 May 26
NGC 3503		5 × 450	5 × 240	2005 Apr. 13
		5 × 120	5 × 60	2009 Mar 16
RCW 87		5 × 450	5 × 240	2005 Apr. 14
	9 × 500	5 × 500	3 × 300	2007 May 24
RCW 98	6 × 500	9 × 120	10 × 60	2007 May 25
	6 × 500	5 × 100	7 × 60	2007 May 26
RCW 99	6 × 500	5 × 120	5 × 60	2007 May 25
Gum 61 †	9 × 500	5 × 200	5 × 100	2007 May 24
Gum 64a†	4 × 500	5 × 120	5 × 60	2007 May 25

Notes. † Part of NGC 6334.

Table 2. Journal of spectroscopic observations.

Star	α(2000)	δ(2000)	Tel.	Date	Wavelength range (Å)	Grid gr./mm	Scale (″/pxl)	Disp. (Å/pxl)	Res. (Å)	Exp. (s)
Bran 186-1	$08^h48^m43\overset{s}{.}14$	–42°54′18.″3	1.6 m	2009 Mar 24	4015–4965	1200	0.56	0.50	5.0	2 × 600
			1.6 m	2009 Mar. 24	4015–4965	1200	0.56	0.50	2.7	1 × 1200
Bran 186-2	08 48 48.14	–42 54 20.9	1.6 m	2009 Mar. 24	4015–4965	1200	0.56	0.50	2.7	2 × 600
			1.6 m	2009 Mar. 24	4015–4965	1200	0.56	0.50	2.7	1 × 1200
Bran 186-3	08 48 39.05	–42 53 54.0	1.6 m	2009 Mar. 24	4015–4965	1200	0.56	0.50	2.7	1 × 1200
			1.6 m	2009 Mar. 29	4015–4965	1200	0.56	0.50	2.7	2 × 1200
Bran 186-4	08 48 35.47	–42 54 31.5	1.6 m	2009 Mar. 26	4015–4965	1200	0.56	0.50	2.7	2 × 1200
Bran 186-5	08 48 43.31	–42 54 33.1	1.6 m	2009 Mar. 26	4015–4965	1200	0.56	0.50	2.7	2 × 1200
NGC 2626-1	08 35 31.44	–40 40 19.1	1.6 m	2009 Mar. 27	4015–4965	1200	0.56	0.50	2.7	1 × 1200
RCW 32-1	08 44 40.33	–41 16 37.9	1.6 m	2009 Mar. 27	4015–4965	1200	0.56	0.50	2.7	3 × 100
RCW 55-1	10 56 38.87	–63 01 02.8	1.6 m	2009 Mar. 25	4015–4965	1200	0.56	0.50	2.7	1 × 1200
			1.6 m	2009 Mar. 26	4015–4965	1200	0.56	0.50	2.7	2 × 1200
			1.6 m	2009 Mar. 29	4015–4965	1200	0.56	0.50	2.7	2 × 1200
RCW 55-2	10 56 40.31	–63 01 04.5	1.6 m	2009 Mar. 25	4015–4965	1200	0.56	0.50	2.7	1 × 1200
			1.6 m	2009 Mar. 26	4015–4965	1200	0.56	0.50	2.7	2 × 1200
			1.6 m	2009 Mar. 29	4015–4965	1200	0.56	0.50	2.7	2 × 1200
RCW 55-3	10 56 32.20	–62 59 58.5	1.6 m	2008 Mar. 08	4000–6000	600	0.51	1.05	5.0	1 × 1200
			1.6 m	2009 Mar. 26	4015–4965	1200	0.56	0.50	2.7	3 × 1200
RCW 55-4	10 56 42.20	–63 01 16.7	1.6 m	2008 Mar. 08	4000–6000	600	0.51	1.05	5.0	1 × 600
			1.6 m	2009 Mar. 25	4015–4965	1200	0.56	0.50	2.7	1 × 1200
			1.6 m	2009 Mar. 29	4015–4965	1200	0.56	0.50	2.7	1 × 1200
RCW 55-5	10 56 40.16	–62 58 46.3	1.6 m	2009 Mar. 25	4015–4965	1200	0.56	0.50	2.7	1 × 1200
			1.6 m	2009 Mar. 25	4015–4965	1200	0.56	0.50	2.7	2 × 1200
RCW 55-6	10 56 27.00	–63 00 00.4	1.6 m	2008 Mar. 08	4000–6000	600	0.51	1.05	5.0	1 × 1200
			1.6 m	2009 Mar. 26	4015–4965	1200	0.56	0.50	2.7	3 × 1200
			1.6 m	2009 Mar. 29	4015–4965	1200	0.56	0.50	2.7	1 × 1200
RCW 55-7	10 56 32.28	–63 00 47.5	1.6 m	2008 Mar. 08	4000–6000	600	0.51	1.05	5.0	1 × 1000
			1.6 m	2009 Mar. 26	4015–4965	1200	0.56	0.50	2.7	3 × 1200
			1.6 m	2009 Mar. 29	4015–4965	1200	0.56	0.50	2.7	1 × 1200
NGC 3503-1	11 01 17.17	–59 51 01.9	1.6 m	2009 Mar. 24	4015–4965	1200	0.56	0.50	2.7	1 × 1200
			1.6 m	2009 Mar. 29	4015–4965	1200	0.56	0.50	2.7	1 × 1200
NGC 3503-2	11 01 17.80	–59 50 30.3	1.6 m	2008 Feb. 01	4000–5000	1200	0.51	0.50	2.7	1 × 1500
			1.6 m	2009 Mar. 26	4015–4965	1200	0.56	0.50	2.7	2 × 1200
NGC 3503-3	11 01 18.24	–59 50 57.8	1.6 m	2009 Mar. 24	4015–4965	1200	0.56	0.50	2.7	1 × 1200
			1.6 m	2009 Mar. 29	4015–4965	1200	0.56	0.50	2.7	1 × 1200
NGC 3503-4	11 01 19.25	–59 50 56.6	1.6 m	2009 Mar. 24	4015–4965	1200	0.56	0.50	2.7	1 × 1200
			1.6 m	2009 Mar. 29	4015–4965	1200	0.56	0.50	2.7	1 × 1200
NGC 3503-5	11 00 59.27	–59 50 30.9	1.6 m	2009 Mar. 26	4015–4965	1200	0.56	0.50	2.7	2 × 1200
RCW 87-1	15 05 09.78	–57 32 18.6	1.6 m	2006 Apr. 24†	3900–7800	300	0.51	2.26	8.8	1 × 1200
			1.6 m	2009 Mar. 26	4015–4965	1200	0.56	0.50	2.7	1 × 1200
			1.6 m	2009 Mar. 29	4015–4965	1200	0.56	0.50	2.7	1 × 1200
RCW 87-2	15 05 36.05	–57 32 58.8	1.6 m	2009 Mar. 29	4015–4965	1200	0.56	0.50	2.7	1 × 1200
RCW 87-3	15 05 15.28	–57 31 25.1	1.6 m	2009 Mar. 29	4015–4965	1200	0.56	0.50	2.7	1 × 1200
RCW 98-1	15 55 39.56	–54 38 36.5	1.6 m	2008 Mar. 07	4000–6000	600	0.51	1.05	5.0	1 × 1200
			1.6 m	2009 Mar. 26	4015–4965	1200	0.56	0.50	2.7	3 × 1000
RCW 98-2	15 55 40.97	–54 41 13.9	1.6 m	2009 Mar. 26	4015–4965	1200	0.56	0.50	2.7	3 × 2000
RCW 98-3	15 55 42.64	–54 39 01.8	1.6 m	2009 Mar. 26	4015–4965	1200	0.56	0.50	2.7	3 × 2000
RCW 99-1	15 59 38.44	–53 45 15.0	1.6 m	2009 Mar. 25	4015–4965	1200	0.56	0.50	2.7	1 × 1200
			1.6 m	2009 Mar. 25	4015–4965	1200	0.56	0.50	2.7	2 × 2400
RCW 99-2	15 59 38.74	–53 44 44.1	1.6 m	2009 Mar. 25	4015–4965	1200	0.56	0.50	2.7	2 × 1800
RCW 99-3	15 59 54.52	–53 44 46.8	1.6 m	2009 Mar. 25	4015–4965	1200	0.56	0.50	2.7	2 × 1800
RCW 99-4	15 59 31.16	-53 44 32.5	1.6 m	2009 Mar. 25	4015–4965	1200	0.56	0.50	2.7	1 × 900
NGC 6334-2	17 19 46.16	–36 05 52.2	0.6 m	2008 Aug. 01	3950–4950	1200	0.56	0.50	2.7	2 × 2000
NGC 6334-5	17 20 05.09	–35 56 41.7	0.6 m	2008 Aug. 04	3950–4950	1200	0.56	0.50	2.7	2 × 2000

Notes. † Archive observation.

Table 3. Spectral classification, photometric data, reddening, and heliocentric distance for individual stars.

Star designation			Spectral type			V	$(B-V)$	$E(B-V)$	A_V	R_V	d (kpc)
Our	2MASS	Simbad	Our	Lit.	Ref						
Bran 186-1	J08484314-4254183	Cl* Trumpler 10 STOCK 724	Cold								
Bran 186-2	J08484813-4254208	Cl* Trumpler 10 STOCK 732	Cold								
Bran 186-3	J08483905-4253539	Cl* Trumpler 10 STOCK 711	B0 V			10.80	0.50	0.76	2.28 ± 0.90	3.00	3.05 ± 1.45
Bran 186-4	J08483546-4254315	Cl* Trumpler 10 STOCK 694	F8:								
Bran 186-5	J08484331-4254330		Cold								
NGC 2626-1	J08353144-4040190	CD-40 4427	B1 V	B1 V	[1]	9.92	0.47	0.70	2.73 ± 0.37	3.90	1.20 ± 0.34
				B1 IV	[2]						
RCW 32-1	J08444032-4116378	HD 74804	B0 V	B0 V	[2]	7.32	0.33	0.59	2.10 ± 0.23	3.56	0.67 ± 0.17
				B4 II	[3]						
				B5 V	[4]						
				B1 V	[5]						
NGC 3503-1	J11011717-5951019		B2 V	B2 V	[1]	11.40	0.20	0.41	1.55 ± 0.33	3.75	2.90 ± 0.80
NGC 3503-2	J11011780-5950302		B0 V	B0 V	[1]	10.49	0.22	0.48	2.10 ± 0.55	4.37	2.88 ± 0.99
NGC 3503-3	J11011823-5950578	Cl Pismis 17 3	B2 V	B2 V	[1]	11.40	0.22	0.43	1.60 ± 0.17	3.73	2.85 ± 0.70
NGC 3503-4	J11011924-5950565	CPD-59 2945s	B2 V	B2 V	[1]	11.37	0.23	0.44	1.62 ± 0.06	3.72	2.78 ± 0.65
NGC 3503-5	J11005926-5950308		B8 V			13.03	0.38	0.49	1.55 ± 0.10	3.14	2.17 ± 0.51
RCW 55-1	J10563886-6301028	VdBH 45c	B0 V	B0 V	[6]	11.51	0.44	0.70	2.07 ± 0.35	2.97	4.66 ± 1.31
RCW 55-2	J10564031-6301044	VdBH 45 F	B2.5 V			13.81	0.55	0.75	2.39 ± 0.16	3.19	4.84 ± 1.18
RCW 55-3	J10563219-6259584	VdBH 45 K	B1 V			12.14	0.48	0.71	2.01 ± 0.28	2.83	4.64 ± 1.23
RCW 55-4	J10564220-6301166	VdBH 45d	O8 V	O6	[7]	10.69	0.45	0.73	2.22 ± 0.50	3.03	4.36 ± 1.42
RCW 55-5	J10564016-6258463		B2.5 V			12.36	0.58	0.78	2.10 ± 0.47	2.69	2.84 ± 0.90
RCW 55-6	J10562699-6300003		B8 IV			13.21	0.51	0.61	1.67 ± 0.32	2.73	2.80 ± 0.77
RCW 55-7	J10563227-6300475	VdBH 45b	B1 V	B1 Vp	[1]	11.31	0.48	0.71	2.13 ± 0.33	3.00	2.99 ± 0.83
RCW 87-1	J15050977-5732186		B4 V			11.61	0.41	0.57	2.30 ± 0.13	4.04	1.39 ± 0.33
RCW 87-2	J15053604-5732587		B9 III			11.84	0.54	0.61	2.31 ± 0.16	3.81	1.06 ± 0.26
RCW 87-3	J15051528-5731251		Cold								
RCW 98-1	J15560198-5440532	HIP 77994	O9 V	O9.5 IV	[2]	10.49	0.47	0.75	2.86 ± 0.11	3.79	2.62 ± 0.62
RCW 98-2	J15554096-5441138	[OM80] 140	O9.5 V			12.41	0.81	1.08	4.52 ± 0.31	4.18	2.61 ± 0.71
RCW 98-3	J15554264-5439018		B2.5 V			12.95	0.57	0.77	2.90 ± 0.12	3.77	2.58 ± 0.61
RCW 99-1	J15593844-5345149		O7 III			13.22	1.69	1.98	6.12 ± 1.30	3.09	3.57 ± 2.29
RCW 99-2	J15593874-5344440		B2 V			12.43	0.47	0.68	2.16 ± 0.51	3.16	3.53 ± 1.17
RCW 99-3	J15595452-5344468		A7: V:								
RCW 99-4	J15593115-5344325		F3 V								
NGC 6334-1	J17194504-3605469	HD 319703B		O6.5 V	[8]	11.47	1.10	1.39	5.42 ± 1.00	3.89	1.62 ± 0.84
NGC 6334-2	J17194616-3605522	HD 319703A	O7 III	O7.5 III	[8]	10.73	1.02	1.31	5.13 ± 0.26	3.92	1.79 ± 0.47
NGC 6334-3	J17205268-3604206	HD 156738		O6.5 III	[8]	9.37	0.86	1.15	3.94 ± 0.24	3.41	1.70 ± 0.44
NGC 6334-4	J17193042-3542362	HD 319699		O5 V	[8]	9.63	0.77	1.07	3.66 ± 0.45	3.42	1.88 ± 0.59
NGC 6334-5	J17200509-3556416	LS 4087	B0.5 V			11.22	1.18	1.42	3.79 ± 0.53	2.67	1.69 ± 0.56
NGC 6334-6	J17205061-3551459	HD 319702		O8 III	[8]	10.13	0.90	1.17	4.00 ± 0.10	3.42	2.19 ± 0.52

References. [1] Herbst (1975), [2] Crampton (1971), [3] Houk (1978), [4] Buscombe (1969), [5] Georgelin et al. (1973), [6] Avedisova & Kondratenko (1984), [7] Georgelin & Georgelin (1970b), [8] Walborn (1982).

Notes. *UBV* stellar photometry for Bran 186, NGC 2626, and RCW 32 from Stock (1984), Denoyelle (1977), and Corben et al. (1972), respectively.

Table 5. Comparison between stellar and nebular properties.

H II region	d (kpc)	$C(\mathrm{H}\beta)$			$\log N_c$ (photons s^{-1})			$F(\lambda 4959)/\mathrm{H}\beta$	Spectral types
		Stars	$\mathrm{H}\gamma/\mathrm{H}\beta$	2.7 GHz	Stars	$\mathrm{H}\beta$	2.7 GHz		
Bran 186	3.05	1.14	1.57		48.02	47.2:		0.16	B0 V
NGC 3503	2.85	0.67	0.58	2.95	48.03	46.56	48.83	0.04	B0 V, 3 × B2 V
RCW 55	4.36	1.07	0.74		48.90	46.82		0.17	B1 V
RCW 87	1.23	2.70	2.89	3.34	45.16	47.44	48.08	0.31	B4 V
RCW 99	3.55	2.97	1.56	2.70	49.36	49.25	48.98	0.28	O7 III, B2.5V
Gum 64a	1.75	2.13			47.77	47.81			B0.5 V